Available online at www.sciencedirect.com
SCIENCE DIRECT®
European Polymer Journal 41 (2005) 3060–3068
EUROPEAN POLYMER JOURNAL
www.elsevier.com/locate/europolj

Isothermal and nonisothermal crystallization kinetics of novel odd–odd polyamide 9 11

Xiaowen Cui, Shengbo Qing, Deyue Yan *

College of Chemistry and Chemical Technology, Shanghai Jiao Tong University, 800 Dongchuan Road, Shanghai 200240, PR China

Received 28 July 2004; received in revised form 19 May 2005; accepted 5 June 2005
Available online 26 July 2005

Abstract

A study on isothermal and nonisothermal crystallization kinetics of odd–odd polyamide 9 11 was carried out by differential scanning calorimetry (DSC). The equilibrium melting temperature of polyamide 9 11 was determined to be 199.1 °C. The Avrami equation was adopted to describe isothermal crystallization of polyamide 9 11. Nonisothermal crystallization was analyzed using both the Avrami relation modified by Jeziorny and the equation suggested by Mo. The isothermal and nonisothermal crystallization activation energies of polyamide 9 11 were determined to be −310.9 and −269.0 kJ/mol using the Arrhenius equation and the Kissinger method, respectively.
© 2005 Elsevier Ltd. All rights reserved.

Keywords: Odd–odd polyamide; Crystallization; Activation energy; Differential scanning calorimetry

1. Introduction

The aliphatic polyamides, known as nylons, have been widely investigated and applied in virtue of their excellent properties including high modulus, eminent toughness, low creep and good temperature resistance [1–5]. Among them, odd–odd polyamides were also well studied because of their special properties such as ferroelectricity and piezoelectricity [2–4]. However, little work was found in the literature about odd–odd polyamides with long alkane segments. Recently, the novel odd–odd polyamides based on undecanedioic acid were synthesized, which have a relatively long CH_2 sequence in the carboxylic acid moiety [5]. For odd–odd nylons excluding the series $(2N-1)(2N+1)$, the neighboring molecular chains cannot establish the full hydrogen bonds based on the trans conformation (Fig. 1a), which is very different from commercial nylons like nylon 11 (Fig. 1b), nylon 10 10 (Fig. 1c) [3,4]. However, odd–odd nylons $(2N-1)(2N+1)$ can form the full effective hydrogen bonds between the close molecular chains because the numbers of the CH_2 units between the diamine moiety and the dicarboxylic acid segment are equal. Among them, nylon 9 11 is an example with long methylene sequences between amide groups. From Fig. 1d, it can be observed that polyamide 9 11 constitutes hydrogen bonds to the neighboring molecular chains and that complete hydrogen bonding is possible. This is different form nylons 10 11 and 11 11. In addition, the polar hydrogen bonded sheet was obtained due to the orientation of the amino and carbonyl groups in molecular chains. Therefore, the novel 9 11 presents a special molecular structure different from other odd, odd–odd and even–even nylons.

* Corresponding author. Fax: +86 21 54741297.
E-mail addresses: cuixiaowen@sjtu.edu.cn (X. Cui), dyyan@sjtu.edu.cn (D. Yan).

0014-3057/$ - see front matter © 2005 Elsevier Ltd. All rights reserved.
doi:10.1016/j.eurpolymj.2005.06.002

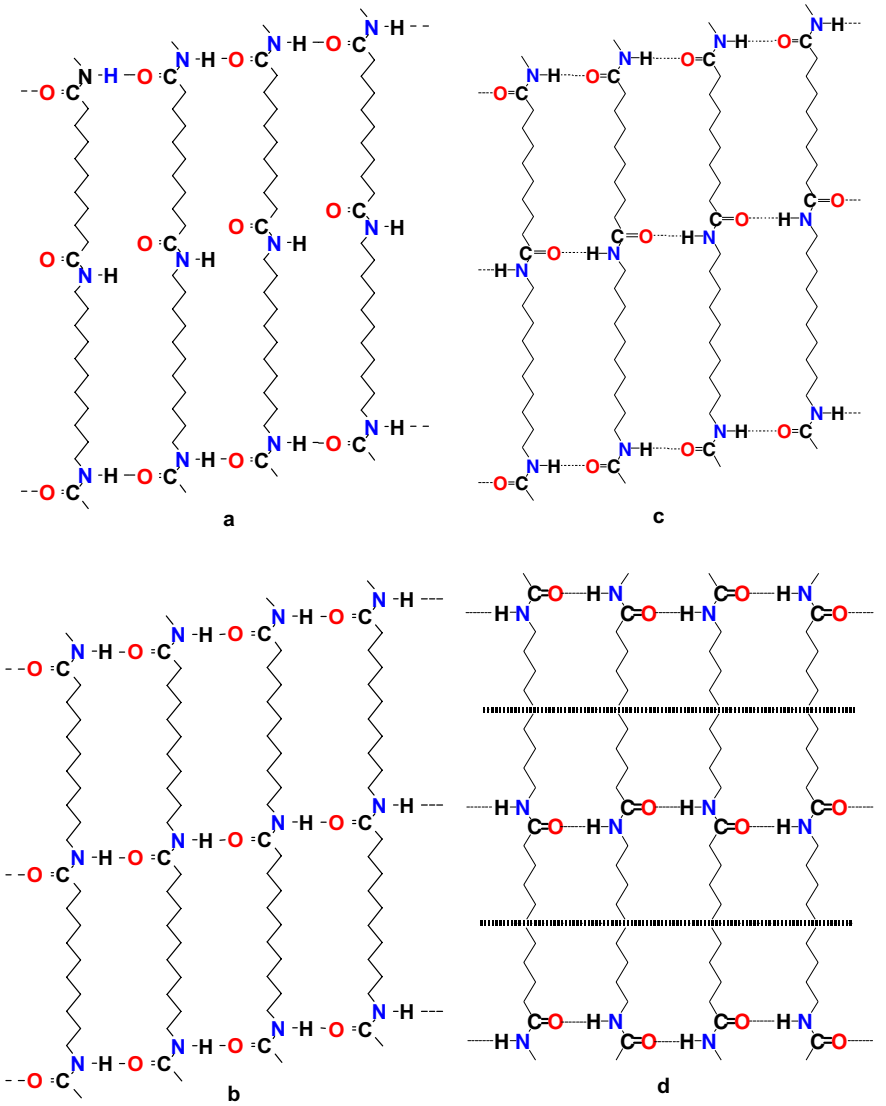

Fig. 1. The scheme of hydrogen bonded sheet of several nylons. (a) Nylon 11 11; (b) Nylon 10 10, (c) Nylon 11; (d) Nylon 9 11. Note that the dashed line in the plane of the sheet is a twofold screw axis which relates the neighboring chains.

On the other hand, the crystallization process of the semi-crystalline thermoplastics is of great practical importance because it exerts a huge effect on the crystal structures, morphologies and properties of the polymer. For example, the procedures of extrusion-molding and film-forming are performed under conditions of isothermal crystallization and nonisothermal crystallization, respectively. Being a new material, it is essential to investigate the crystallization kinetics and melting behavior of polyamide 9 11 for its potential applications in the future, although similar studies of other polyamides were performed in the past [6–9]. In this study, the melt behavior and the crystallization kinetics of polyamide 9 11 were studied by DSC.

2. Experimental

2.1. Materials and preparation

Odd–odd polyamide 9 11 was synthesized by polycondensation of diaminononane with undecanedioic acid [5]. The intrinsic viscosity of polyamide 9 11 was 0.82 dl/g determined in dichloroacetic acid at 25 °C. The sample was kept in a vacuum oven for 12 h before use.

2.1.1. Differential scanning calorimetry

Isothermal and nonisothermal crystallization kinetics were determined using a Perkin-Elmer Pyris-1 differential

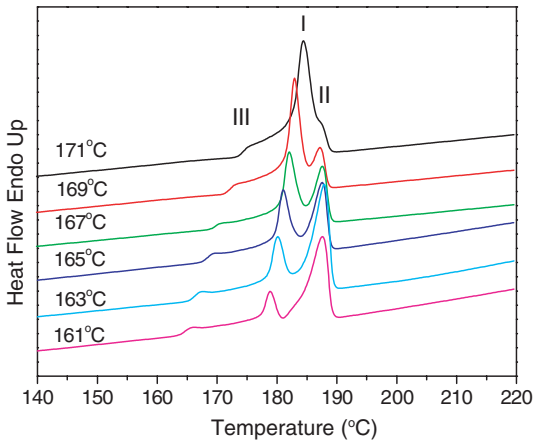

Fig. 2. The DSC melting thermograms of odd–odd polyamide 9 11 after isothermal crystallization at the specified temperatures.

scanning calorimeter under nitrogen. The temperature was calibrated with indium. All DSC sample weights were in the range of 5–8 mg.

2.1.2. Isothermal and nonisothermal crystallization process

Isothermal crystallization process: The samples were heated to 220 °C at 20 °C/min and kept at this temperature for 10 min to eliminate the residual crystals. Then they were cooled to the designated crystallization temperatures (T_c) at −100 °C/min for isothermal crystallization, which were six different temperatures in the range of 161–171 °C (Fig. 4). Finally, the samples were cooled to room temperature at 10 °C/min and heated to 220 °C at 10 °C/min for determination of the equilibrium melting temperature (Fig. 2).

Nonisothermal crystallization process: The samples were heated to 220 °C at 20 °C/min and kept at this temperature for 10 min to eliminate the residual crystals. Then they were cooled to room temperature at different cooling rates, −2.5, −5, −10, −20 and −40 °C/min, respectively (Fig. 9).

3. Results and discussion

3.1. Isothermal crystallization analysis

3.1.1. Equilibrium melting temperature

Fig. 2 shows the DSC thermograms of the polyamide 9 11 samples melt-crystallized at different T_cs (161–171 °C). All the DSC curves exhibit double melting peaks, peak I and peak II, on the high temperature side. Peak I rises in size and tends to approach higher temperature as the T_c increases. Peak II becomes smaller at the same time, but its position remains at 188 °C on the temperature scale. The double melting peaks of polyamide 9 11 can be attributed to recrystallization phenomena during the continuous heating process [10]. Peak I originates from melting of the crystal formed at each T_c, while peak II corresponds to the more perfect crystals. As temperature increases, the crystal grows more and more perfect, which makes peak I shift to the high temperature side. Upon heating, the less stable crystals melt at a supercooled state. Meanwhile, recrystallization occurs and better crystals are built up. Finally, the perfectly recrystallized material melts always at the same temperature, irrespective of the T_c. In addition, peak III exists in all the samples at 4 °C above the T_c and moves more sharply to higher temperature as the T_c increases. Peak III is attributed to the annealing effect at the T_c. A small part of amorphous polymer between the bundles of lamella forms crystallites and the defective crystals aggregate in the boundary layer. This produces the melting peak III at a few degrees above the T_c [11]. Therefore, peak I is associated with the T_c and appropriate for the determination of equilibrium melting temperature (T_m^0).

As an important parameter characteristic of the crystal of the flexible linear polymer, T_m^0 illustrates the melting temperature (T_m) of an infinitely extended crystal and can be obtained from the procedure suggested by Hoffman and Weeks [12]. According to the theoretical considerations by Hoffman and Weeks, the dependence of T_m and T_c is expressed as follows:

$$T_m = \frac{T_c}{2\beta} + T_m^0\left[1 - \frac{1}{2\beta}\right] \quad (1)$$

where β is the lamella thickening factor, which indicates the ratio of the thickness of the mature crystal L_c to that of the initial crystal L_c^*. Fig. 3 presents the plot of T_m versus T_c. An equilibrium melting temperature of 199.1 °C was obtained by means of the extrapolation of the resulting straight line to the line $T_m = T_c$.

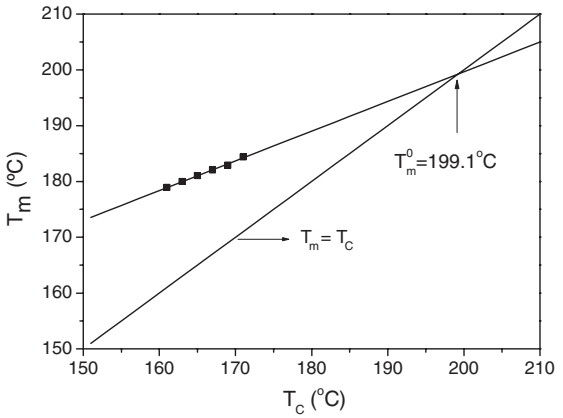

Fig. 3. The change of the melting temperature taken as a function of the crystallization temperature for polyamide 9 11.

3.1.2. Isothermal crystallization kinetics analysis based on Avrami equation

The DSC thermograms of the samples in the isothermal crystallization process are shown in Fig. 4. The crystallization process is usually treated as a composition of two stages: the primary crystallization stage and the secondary crystallization stage. The crystallization process is very temperature dependent. The Avrami equation (Eq. (2)) was utilized to analyze the isothermal crystallization process [13]:

$$X(t) = 1 - \exp(-K \cdot t^n)$$
$$\log\{-\ln[1 - X(t)]\} = n \cdot \log t + \log K \quad (2)$$

where $X(t)$ is the degree of crystallinity at time t, n is the Avrami exponent and K is the isothermal crystallization rate parameter. The plots of $\log\{-\ln[1-X(t)]\}$ versus $\log t$ are presented in Fig. 5. It was found that each curve is composed of two linear sections, indicating the existence of secondary crystallization. The spherulite impingement in the later stage of the crystallization process results in the deviation of the plots from the straight line [14]. The Avrami exponent n and the isothermal crystallization rate parameter K were extracted by performing the least square fit to the Avrami plots and

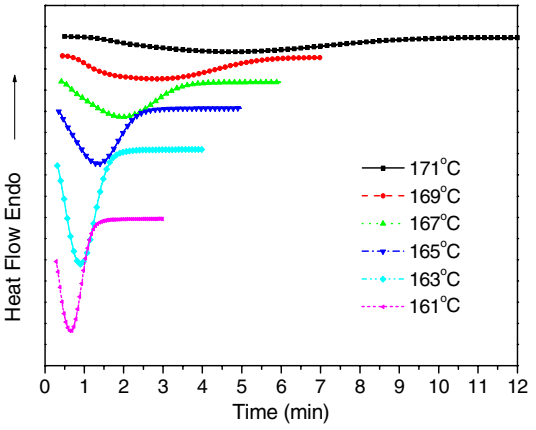

Fig. 4. Heat flow versus time during the isothermal crystallization of polyamide 9 11 at the specified crystallization temperatures by DSC.

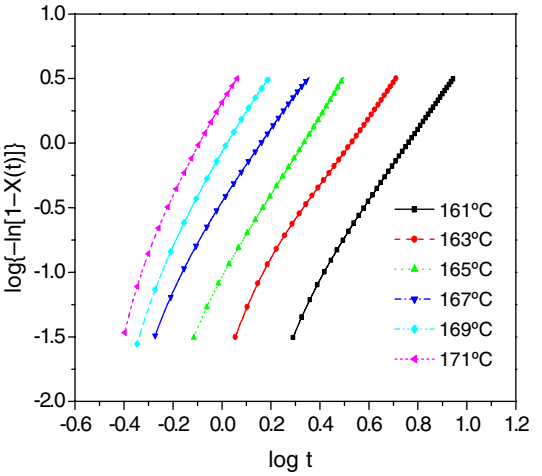

Fig. 5. The plots of $\log\{-\ln[1 - X(t)]\}$ versus $\log t$ at the indicated temperatures for the isothermal crystallization of polyamide 9 11.

listed in Table 1. The Avrami exponent n is in the range of 2.78–2.98, relying on T_c. The results indicate that the spherulite growth mode of polyamide 9 11 is mainly in three-dimensional orientation with thermal nucleation, since no nucleation agent was added to the homopolymer sample of polyamide 9 11. The isothermal crystallization rate parameter K decreases as the T_c increases (Table 1).

The crystallization half-time ($t_{1/2}$) is defined as time at which the crystallinity degree is 50% of the maximum achievable crystallinity, and can be calculated from the measured kinetics parameters,

$$t_{1/2} = \left(\frac{\ln 2}{K}\right)^{1/n} \quad (3)$$

The rate of crystallization G is defined as the reciprocal of $t_{1/2}$, e.g. $G = \tau_{1/2} = (t_{1/2})^{-1}$. It is observed that the rate of crystallization of polyamide 9 11 is higher than that of polyamide 10 10 ($\tau_{1/2} = 0.1$–$1.2\ \mathrm{min}^{-1}$) under the same supercooling condition, though polyamides 9 11 and 10 10 have the same density of hydrogen bonds [15]. Most likely, this is related to the higher degree of symmetry of polyamide 9 11 with respect to polyamide

Table 1
Collection of the parameters for isothermal crystallization of polyamide 9 11

T_c (°C)	161	163	165	167	169	171
n	2.98	2.92	2.89	2.83	2.80	2.78
K (min^{-1})	2.2	0.78	0.32	0.091	0.034	0.0062
t_{max} (min)	0.66	0.91	1.38	1.96	2.77	4.68
$t_{1/2}$ (min)	0.74	0.94	1.26	1.90	2.92	5.03
$\tau_{1/2}$ (min^{-1})	1.35	1.06	0.79	0.53	0.34	0.20
U^* (J/mol)	41,910.08	41,636.37	41,368.66	41,106.76	40,850.49	40,599.65

10 10 (see Fig. 1c and d). However, the crystallization rate of polyamide 9 11 is much lower than that for polyamide 6 and polyamide 66 ($\tau_{1/2} = 12\ \mathrm{min}^{-1}$ and $144\ \mathrm{min}^{-1}$) [16]. Therefore, the crystallization rates of polyamides have no direct relationship with their concentration of hydrogen bonds. Data on the time needed for maximum crystallinity t_{max} can be achieved from the heat-flow curves in Fig. 4. The isothermal crystallization parameters n, K, t_{max}, $t_{1/2}$ and $\tau_{1/2}$ are listed in Table 1. The value of t_{max} can also be calculated from the following equation [17]:

$$t_{max} = \left(\frac{n-1}{n \cdot K}\right)^{1/n} \tag{4}$$

which is deduced by Lin from the condition where $dQ(t)/dt = 0$, and $Q(t)$ is the heat-flow rate.

3.1.3. Crystallization activation energy (ΔE) for isothermal crystallization

Assuming that the crystallization process of polyamide 9 11 is thermally activated, the crystallization rate parameter K can be described as the following Arrhenius form [18]:

$$K^{1/n} = k_0 \cdot \exp\left(\frac{-\Delta E}{R \cdot T_c}\right)$$
$$\frac{1}{n} \cdot \ln K = \ln k_0 - \frac{\Delta E}{R \cdot T_c} \tag{5}$$

where k_0 is the temperature-independent pre-exponential factor, R is the gas constant and ΔE is the crystallization activation energy. The slope coefficient of the plot of $(1/n)\ln K$ versus $1/T_c$ is used to calculate the ΔE (Fig. 6). The value of ΔE for the isothermal crystallization process of polyamide 9 11 is -310.9 kJ/mol.

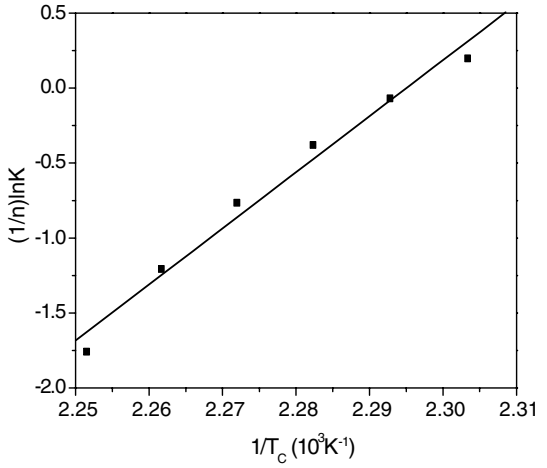

Fig. 6. The variation of the Avrami parameters $(1/n)\ln K$ as function of $1/T_c$ for the acquisition of the isothermal crystallization activation energy.

The Turnbull–Fisher expression describes the spherulite growth rate and is given by [19]:

$$\ln G = \ln G_0 - \frac{\Delta E^*}{k \cdot T_c} - \frac{\Delta F^*}{k \cdot T_c} \tag{6}$$

where G is the spherulite growth rate, G_0 is a pre-exponential factor, k is the Boltzmann constant, T_c is crystallization temperature, ΔE^* is the free energy of activation for transporting a chain segment from the supercooled state to the crystalline phase and ΔF^* is the free energy of formation of a nucleus of critical size. At relatively low temperature, the transportation term, $-\Delta E^*/kT_c$, declines rapidly. When T_c is close to T_g, the transportation term should be dominant for the crystallization rate. At relatively high temperature, that is, T_c approaches T_m, the nucleation term, $-\Delta F^*/kT_c$, decreases quickly, and it is of primary importance for the crystallization rate in the melt crystallization process. The phenomenon results in the presence are explained as the presence of a maximum in the behavior of the growth rate versus temperature. In our experiment, the values of T_c are in the range of 161–171 °C, and therefore the transportation term is negligible in the isothermal crystallization process for polyamide 9 11. The following equation is obtained:

$$\ln G = \ln G_0 - \Delta F^*/k \cdot T_c \tag{7}$$

where the crystallization rate is controlled by the nucleation term and derived by Hoffmann as follows:

$$\ln G = \ln G_0 - \frac{\chi \cdot T_m^0}{T_c^2 \cdot (T_m^0 - T_c)} \tag{8}$$

where T_m^0 is the equilibrium melting temperature and χ is the parameter dealing with the heat of fusion and the interfacial free energy.

Based on Eqs. (2), (4) and (8), the following equation was obtained by Lin [17]:

$$\log t_{max} = B - \frac{C}{2.303 \cdot T_c^2 \cdot \Delta T} \tag{9}$$

where B and C are constants, and ΔT is the degree of supercooling ($\Delta T = T_m^0 - T_c$). Eq. (9) is used to verify whether polyamide 9 11 can be described by the Avrami equation in the isothermal crystallization process. If so, the plot of $\log t_{max}$ versus $1/(T_c^2 \Delta T)$ should be a straight line. From Fig. 7, it can be observed that the plot shows an excellent linear relation indeed.

3.1.4. Spherulite growth analysis

The famous Lauritzen–Hoffmann equation was applied to describe the spherulite growth rate in the isothermal crystallization process of the homopolymer for higher degrees of supercooling [20]. That is:

$$G = G_0 \cdot \exp\left[-\frac{U^*}{R \cdot (T_c - T_\infty)}\right] \exp\left[-\frac{K_g}{T_c \cdot \Delta T \cdot f}\right] \tag{10}$$

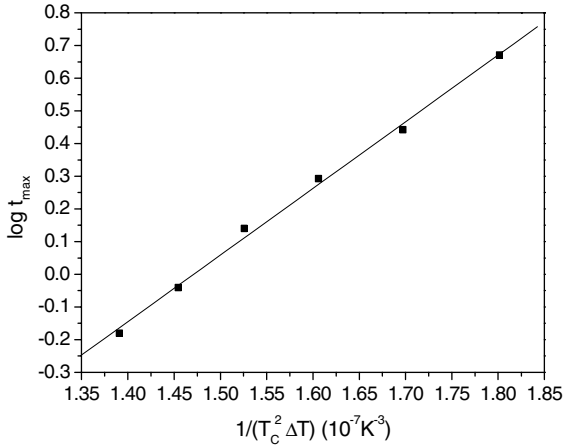

Fig. 7. The plot of $\log t_{max}$ versus $1/(T_c^2 \Delta T)$ for odd–odd polyamide 9 11 in the isothermal crystallization.

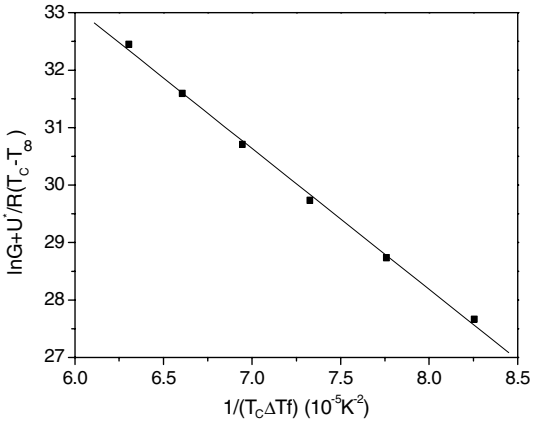

Fig. 8. $\ln G + U^*/R(T_c - T_\infty)$ versus $1/(T_c \Delta Tf)$ for odd–odd polyamide 9 11.

where U^* is the transport activation energy, T_∞ is a hypothetical temperature below which all viscous flow ceases ($T_\infty = T_g - 30$), K_g is a nucleation parameter, ΔT is the degree of supercooling and f is a correction factor accounting for the variation in the bulk enthalpy of fusion per unit volume with temperature, $f = 2T_c/(T_m^0 + T_c)$.

The transport activation energy U^* in Eq. (10) can be calculated with the Williams–Landel–Ferry equation [21]:

$$U^* = \frac{C_1 \cdot T_c}{C_2 + T_c - T_g} \tag{11}$$

where C_1 and C_2 are constants, which are generally assumed to be 4120 cal/mol and 56.1 K, respectively [22]. The calculated values are listed in Table 1.

The double logarithmic relation of Eq. (10) is presented:

$$\ln G + \frac{U^*}{R \cdot (T_c - T_\infty)} = \ln G_0 - \frac{K_g}{T_c \cdot \Delta T \cdot f} \tag{12}$$

The plot of $\ln G + U^*/R(T_c - T_\infty)$ versus $1/T_c \Delta T f$ yields a perfectly straight line in Fig. 8, indicating that the L–H equation can describe the crystallization process of polyamide 9 11. The value of K_g is determined from the slope of the plot, and appears to be 2.5×10^5 K^2 for polyamide 9 11.

3.2. Nonisothermal crystallization analysis

3.2.1. Nonisothermal crystallization kinetics analysis from Avrami equation modified by Jeziorny

The crystallization exotherms of polyamide 9 11 at various cooling rates, Φ, are shown in Fig. 9. The peak temperature (T^*), where the crystallization rate achieves its maximum, shifts to the low temperature region when

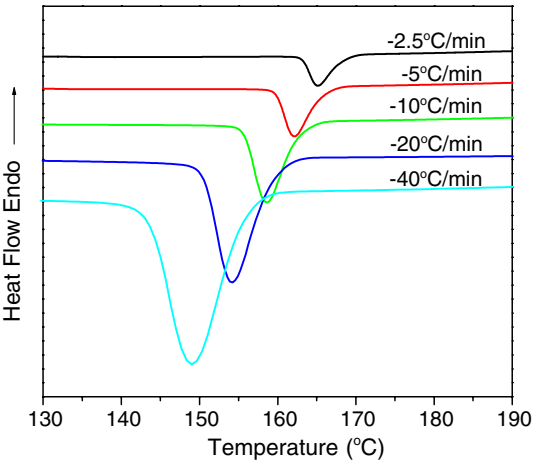

Fig. 9. The DSC thermograms of nonisothermal crystallization of polyamide 9 11 at the indicated cooling rates.

the cooling rate increases. The crystallization enthalpies, ΔH_c, and the T^* at different cooling rates are listed in Table 2.

Fig. 10 depicts the temperature-dependence of the crystallinity degree calculated from the information of Fig. 9. A series of reversed S-shaped curves was observed. During the nonisothermal crystallization process, T_c, T, and crystallization time (t) are related as follows [23]:

$$t = \left| \frac{T_0 - T}{\Phi} \right| \tag{13}$$

where T_0 is the initial temperature at which crystallization starts ($t = 0$). According to Eq. (13), the time-dependence of the crystallinity $X(t)$ can be obtained in Fig. 11. The time, t_{max}, at T^* is determined from

Table 2
The values of T^*, t_{max} and ΔH_c for the nonisothermal crystallization of odd–odd polyamide 9 11

Φ (°C/min)	−2.5	5	10	20	40
T^* (°C)	165.21	162.20	158.56	154.29	149.06
t_{max} (min)	3.47	1.94	1.14	0.63	0.33
ΔH_c (J/g)	−57.331	−56.990	−49.945	−52.468	−51.530

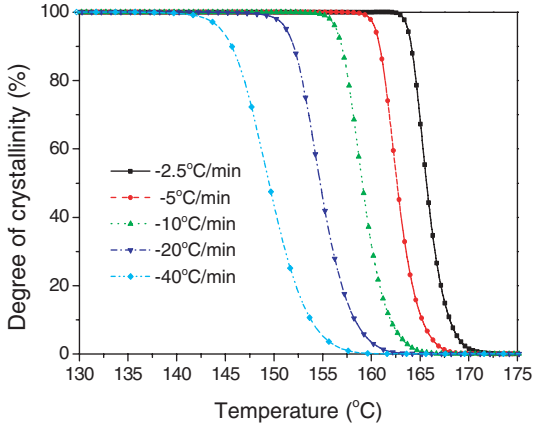

Fig. 10. The crystallinity degree of polyamide 9 11 in the nonisothermal crystallization taken as a function of the T_c at the different cooling rates.

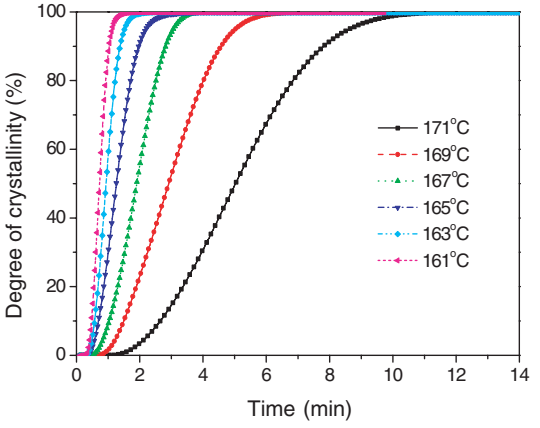

Fig. 11. The time-dependence of the crystallinity degree of polyamide 9 11 for the nonisothermal crystallization with the different cooling rates.

Eq. (13) and listed in Table 2. The half-time, Z, of nonisothermal crystallization was achieved in Table 3.

Based on the assumption that the T_c is constant, the Avrami relation between the crystallinity degree and the crystallization time was adapted to describe the nonisothermal crystallization by Mandelken [24]:

$$X(t) = 1 - \exp[-Z_t \cdot t^n]$$
$$\log\{-\ln[1 - X(t)]\} = n \cdot \log t + Z_t \quad (14)$$

Z_t is the rate parameter in the nonisothermal crystallization process. In order to eliminate the effect of the cooling or heating rate $\Phi = dT/dt$, the rate parameter characteristic of the kinetics of nonisothermal crystallization was modified by Jeziorny [25]:

$$\log Z_c = \frac{\log Z_t}{\Phi} \quad (15)$$

With drawing the plot of $\log\{-\ln[1 - X(t)]\}$ versus $\log t$ (Fig. 12), the values of n and Z_t were determined from the slopes and intercepts, respectively (Table 3). The Z_c was calculated from Eq. (15). From Fig. 12, it was found that all the curves can be subdivided into the following two sections: the primary crystallization stage and the secondary one. At the primary stage, the Avrami exponent, $n_1 > 4$, implies that the mode of nucleation and growth of polyamide 9 11 in the nonisothermal crystallization process is more complicated than that in the isothermal crystallization process. From the obtained Avrami exponent, it is difficult to give a straight explanation with a physical meaning. At the secondary

Table 3
The parameters of n, Z_t and Z_c from the Avrami equation at the two stages of nonisothermal crystallization of odd–odd polyamide 9 11

Φ (°C/min)	Primary crystallization stage			Secondary crystallization stage		
	n_1	Z_{t1}	Z_{c1}	n_2	Z_{t2}	Z_{c2}
2.5	5.16	1.5×10^{-3}	7.4×10^{-2}	3.19	3.7×10^{-2}	0.27
5	5.38	2.7×10^{-2}	0.49	3.22	0.26	0.76
10	5.29	0.43	0.92	3.18	1.34	1.03
20	5.28	10.16	1.12	2.05	5.99	1.09
40	4.35	97.72	1.12	2.20	20.26	1.08

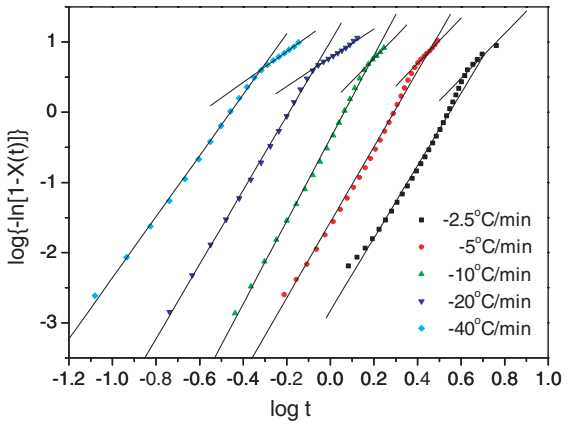

Fig. 12. The plots of $\log\{-\ln[1 - X(t)]\}$ taken as a function of $\log t$ in the nonisothermal crystallization process of polyamide 9 11.

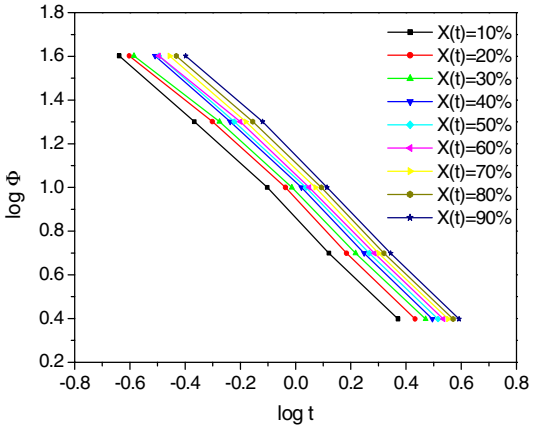

Fig. 13. The plots of $\log\Phi$ versus $\log t$ for the different crystallinity degree for the nonisothermal crystallization of polyamide 9 11.

crystallization stage, the Avrami exponent, $n_2 = 2.20$–3.20, indicates that the mode of nucleation and growth is still the three-dimensional space extension.

3.2.2. Nonisothermal crystallization kinetics analysis by a new equation

Recently, a convenient kinetics approach by combining the Avrami equation with the Ozawa relation was adapted by Mo to describe the nonisothermal crystallization [23]:

$$\log Z_t + n \cdot \log t = \log K(t) - m \cdot \log \Phi$$

$$\log \Phi = \frac{1}{m} \log[K(t)/Z_t] - \frac{n}{m} \log t$$

Assuming $F(T) = [K(T)/Z_t]^{1/m}$, and $a = n/m$, the final form of the new equation can be obtained:

$$\log \Phi = \log F(T) - a \cdot \log t \tag{16}$$

where $F(T)$ is the kinetics parameter referring to the value of the cooling rate chosen at a fixed crystallization time when the measured system contains to a certain degree of crystallinity. $F(T)$ has a definite physical meaning. The parameter a is the ratio of the Avrami exponent n to the Ozawa exponent m. At a certain crystallinity degree of polyamide 9 11, the plots of $\log\Phi$ versus $\log t$ are presented in Fig. 13. The least square fit of the data points gives a series of lines. The parameters $F(T)$ and a in Eq. (16) were determined from slopes and intercepts of the fitted lines (Table 4). The values of $F(T)$ continuously increase with increasing crystallinity, while the values of the parameter a approximately remains constant. Therefore, a relatively high cooling rate should be selected in order to achieve a high degree of crystallinity at a fixed crystallization time. It was observed that Mo's equation can be used to analyze the nonisothermal crystallization kinetics of polyamide 9 11 and gives good results.

3.2.3. Crystallization active energy (ΔE) for nonisothermal crystallization

The crystallization activation energy of a nonisothermal crystallization process was given by Kissinger considering the effect of the changing cooling rate Φ in the nonisothermal crystallization [26]:

$$\frac{\mathrm{d}[\ln(\Phi/T^{*2})]}{\mathrm{d}(1/T^*)} = -\frac{\Delta E}{R} \tag{17}$$

where R is the gas constant and T^* is the peak temperature of the exotherms in Fig. 9. The plot of $\ln(\Phi/T^{*2})$ versus $1/T^*$ is presented in Fig. 14 and the crystallization activation energy of polyamide 9 11, obtained from the slope of the least square fitted line, is −269.0 kJ/mol.

Table 4
The values of a and $F(T)$ from Eq. (16) at a certain degree of crystallinity for odd–odd polyamide 9 11

$X(t)$ (%)	10	20	30	40	50	60	70	80	90
a	1.20	1.17	1.15	1.21	1.20	1.18	1.20	1.21	1.23
$F(T)$	7.12	8.40	9.06	10.11	10.59	11.00	11.74	12.48	13.53

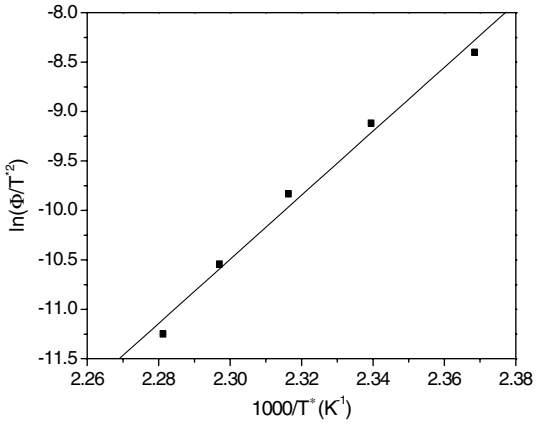

Fig. 14. The variation of $\ln(\Phi/T^{*2})$ taken as a function of $1/T^*$ for nonisothermal activation energy of polyamide 9 11.

4. Conclusion

Polyamide 9 11 has been chosen to investigate the melt behavior and crystallization kinetics in isothermal and nonisothermal crystallization process. The equilibrium melting point of polyamide 9 11 was determined to be 199.1 °C by applying Hoffmann–Weeks method. Isothermal crystallization of polyamide 9 11 was described by the Avrami equation, which slightly tends to deviate from the straight line, indicating the existence of secondary crystallization caused by spherulite impingements. Nonisothermal crystallization of the polyamide under consideration was investigated by two methods: The Avrami method modified by Jeziorny and the relation deduced by Mo. From the analysis by the Avrami method, it can be concluded that two crystallization stages exist in the nonisothermal crystallization process. At the primary stage, the mode of nucleation and growth is very complicated. At the secondary stage, the mode of nucleation and growth is a three-dimensional process. Mo's equation can also be used to describe the nonisothermal crystallization process. The activation energies for the isothermal and nonisothermal crystallization processes are −310.9 and −269.0 kJ/mol, respectively.

Acknowledgment

This work is sponsored by the National Natural Science Foundation of China (Nos. 20274024 and 50233030).

References

[1] Kohan MI. Nylon plastics handbook. Munich: Carl Hanser Verlag; 1995 [chapter 10].
[2] Bermúdez M, León S, Bou J, Muñoz-Guerra S. Macromol Chem Phys 1999;200:2065.
[3] Kinoshita Y. Die Makromol Chem 1959;33:21.
[4] Kinoshita Y. Die Makromol Chem 1959;33:1.
[5] Cui XW, Li WH, Yan DY. Polym Int 2004;53:1729.
[6] Srinivas S, Bahu JR, Riffle JS, Wilkes GL. Polym Eng Sci 1997;37:568.
[7] Srimoaon P, Dangseeyun N, Supaphol P. Eur Polym J 2004;40:599.
[8] Li YJ, Zhang GS, Zhu XY, Yan DY. J Appl Polym Sci 2003;88:1311.
[9] Li YJ, Zhu XY, Yan DY. Polym Eng Sci 2000;40:1989.
[10] Li YJ, Zhu XY, Tian GH, Yan D, Zhou EL. Polym Int 2001;50:677.
[11] Liu M, Zhao Q, Wang Y, Zhang C, Mo Z, Cao S. Polymer 2003;44:2537.
[12] Hoffman J, Weeks J. J Res Natl Bur Stand 1962;A66:13.
[13] Avrami M. J Chem Phys 1940;8:212.
[14] Liu S, Yu Y, Zhang H, Mo Z. J Appl Polym Sci 1998; 70:2371.
[15] Liu J, Mo Z. Chin Polym Bull 1991;4:199.
[16] Ziabicki A. Appl Polym Symp 1967;6:1.
[17] Lin C. Polym Eng Sci 1983;23:113.
[18] Cebe P, Hong S. Polymer 1986;27:1183.
[19] Turnbull D, Fisher J. J Chem Phys 1949;17:71.
[20] Lauritzen JI, Hoffman JD. J Appl Phys 1973;44:4340.
[21] Williams ML, Landel RF, Ferry JD. J Am Chem Soc 1955;77:3701.
[22] Zhong ZK, Guo QP. J Polym Sci Part B: Polym Phys 1999;37:2726.
[23] Zhang Q, Zhang Z, Zhang H, Mo Z. J Polym Sci Part B: Polym Phys 2002;40:1784.
[24] Fava RA. Methods of experimental physics, vol. 16, Part B. New York: Academic; 1980.
[25] Jeziorny A. Polymer 1978;19:1142.
[26] Kissinger HE. J Res Natl Bur Stand 1956;57:217.